Defence Science Journal, Vol. 75, No. 6, November 2025, pp. 742-750, DOI : 10.14429/dsj.20759

Determination of Suitable Structural Characteristics of a Muzzle Device Improving the Stability of an Assault Rifle During Short Burst Firing

Dung Van Nguyen[#], Viet Quy Bui[#,*], Trung Viet Nguyen[#] and Huy Quang Mai[$]

[#]*Faculty of Special Equipment, Le Quy Don Technical University, 236 Hoang Quoc Viet Street, Ha Noi - 100 000, Viet Nam*
[$]*Le Quy Don Technical University, 236 Hoang Quoc Viet Street, Ha Noi - 100 000, Viet Nam*
[*]*E-mail: buiquyviet@lqdtu.edu.vn*

ASTRACT

This paper presents a method for determining the optimal structural characteristics of a muzzle brake compensator to enhance the firing stability of automatic assault rifles during short bursts. Utilizing the principle of independent force action in mechanics, the rifle is modeled as a multi-body system with rigid bodies and concentrated masses, assuming forces acting on the gun, including the shooter's visco-elastic coupling, are independent. The method focuses on minimizing muzzle deflection at the moment a bullet exits the barrel by accurately determining the structural characteristics - α_1, α_y and α_z - which quantify how the gas reaction force from propellant gases generates compensatory impulses along the axial and lateral axes. Theoretical analysis involves solving nonlinear differential equations based on Lagrange's formulation and using internal ballistic data to simulate gun motion and optimize device parameters. Experimental validation, conducted with specialized equipment, demonstrates strong correlation between calculated and observed values (with errors below 9.8 %), confirming that a well-designed muzzle device can significantly reduce recoil and enhance the overall stability and accuracy of automatic weapons.

Keywords: Structural characteristics; Muzzle device; Muzzle displacement; Assault rifle stability; Independent action

NOMENCLATURE

F_{ax}	: Gas port reaction force in the OX direction
F_{az}	: Gas port reaction force in the OZ direction
F_{bb}	: Force of powder gas on the barrel bottom
R_c	: Resistive force acting on the piston
F_k	: Force of powder gas on the gas chamber
F_{mdx}	: Muzzle device reaction force in the OX direction
F_{mdy}	: Muzzle device reaction force in the OY direction
F_{mdz}	: Muzzle device reaction force in the OZ direction
F_{hx}	: Hand reaction force in the OX direction
F_{hy}	: Hand reaction force in the OY direction
F_{hz}	: Hand reaction force in the OZ direction
F_{shx}	: Shoulder reaction force
Π_{sp}	: Force of return spring
m_1	: Effective mass of the shooter
K	: Stiffness coefficient
C	: Viscous coefficient
m_2	: Mass of gun body
m_3	: Bolt carrier group mass
q_1	: Translational movements of object 1 along the axis O_0X_0
q_2	: Translational movements of object 1 along the axis O_0Y_0
q_3	: Translational movements of object 1 along the axis O_0Z_0
q_4	: Rotational movements of object 2 around the axis O_1X_1
q_5	: Rotational movements of object 2 around the axis O_1X_1
q_6	: Rotational movements of object 2 around the axis O_1Z_1
q_7	: Translational movements of object 3 compared to object 2
T	: Total kinetic energy of the mechanical system
T_1	: Kinetic energy of object 1
T_2	: Kinetic energy of object 2
T_3	: Kinetic energy of object 3
$\dot{\vec{R}}_i$	: Displacement velocity vector of the mass center of *i*-th object in the fixed coordinate system
$M]_i^{RR}$	: Translational mass matrix of *i*-th object
$\vec{\omega}_i$	: Angular velocity vector of *i*-th object in the fixed coordinate system
$[A]_{i0}$	: Absolute rotation matrix of dynamic coordinate system O_i(i=1÷3)
$[J]_i$	: Inertia tensor of *i*-th object concerning coordinate system O_i
δW	: Total possible work of the whole system
$\delta W(F_{bb})$	: Possible work of the gunpowder gas force on the bottom of the barrel
$\delta W(F_{ed})$	: Possible work of the force of the gas extraction device

Received : 13 February 2025, Revised : 28 May 2025
Accepted : 20 June 2025, Online published : 06 November 2025

$\delta W(F_{md})$: Possible work of the force created by the muzzle device
$\delta W(\Pi_{sp})$: Possible work of the return spring force
$\delta W(P_G)$: Possible work of gravity
$\delta W(F_{sh})$: Possible work of the force acting by the shooter
$\delta W(R_p)$: Possible work due to the force resisting the piston movement
$\delta W(M_2)$: Possible work due to the torque acting on the barrel groove
Q_j : Generalized force
$\vec{r}_i$: Vector determines the point where the force is applied
$\vec{q}\ iT)$: Movement of the muzzle point of the assault rifle without using the muzzle device
$\vec{q}'(iT)$: Displacement of the muzzle induced solely by the muzzle device force
m_g : Mass of the rifle with the muzzle device
M_{md} : Mass of the muzzle device
$\vec{q}_m$: Vector of translational displacements of the muzzle
$[M]$: Mass matrix
$[C]$: Damping matrix
$[K]$: Stiffness matrix
l_{O_2} : Distance from the point of shoulder rest to the center of the gun mass
l_{md} : Distance from the point of shoulder rest to the muzzle point
J_g^{yy} : Moment of inertia about the OY-axis through the firearm's center of mass
J_g^{zz} : Moment of inertia about the OZ-axis through the firearm's center of mass
C_x : Damping coefficients of the shooter's shoulder along the OX-axis
C_{hy} : Damping coefficients of the shooter's hand along the OY-axis
C_{hz} : Damping coefficients of the shooter's hand along the OZ-axis
K_x : Stiffness coefficients of the shooter's shoulder along the OX-axis
K_{hy} : Stiffness coefficients of the shooter's hand along the OY-axis
K_{hz} : Stiffness coefficients of the shooter's hand along the OZ-axis
α_T : Structural characteristic of the muzzle device along the OX-axis
α_y : Structural characteristic of the muzzle device along the OY-axis
α_z : Structural characteristic of the muzzle device along the OZ-axis
R_x : Reaction force of the gas flowing out of the muzzle
T_0 : Duration of the shot cycle
t_f : Impact duration of the muzzle force
J_f : Impulse of the muzzle device
ξ : Moment the bullet passes through the muzzle cross-section

1. INTRODUCTION

Automatic submachine guns currently in service often demonstrate inadequate firing accuracy compared to the technical potential of modern firearms[1-6]. This limitation stems primarily from dynamic instabilities during automatic fire, caused by complex interactions between the weapon's mechanical components, the shooter, and external force factors. These interactions result in deviations from the intended line of fire, leading to significant shot dispersion. While several approaches have been proposed to mitigate such instability- such as magnetorheological dampers[7], reverse jet flow mechanisms[8-9], elastic recoil-absorbing components[10-11], and active shock absorbers[12], these typically require substantial alterations to the weapon's original design, limiting their practical applicability.

In contrast, passive stabilization methods, particularly through the use of muzzle devices, offer a promising alternative. These devices exploit the energy of propellant gases escaping from barrel to produce compensatory forces that reduce muzzle deflections without requiring fundamental changes to the firearm's structure. Although previous studies have investigated the effects of muzzle devices on gas dynamics, recoil impulses, and barrel behavior, a systematic approach to determine the optimal structural characteristics of these devices remains insufficiently explored[13-28].

This work addresses that gap by proposing a dynamic modeling framework to identify the structural parameters of muzzle devices that enhance firing stability. By representing the firearm as a multi-body system - with rigid components and independent force inputs - the study applies the principle of independent force action to derive key coefficients, denoted as α_T, α_y and α_z. These parameters define how the muzzle device translates the propellant gas reaction force into directional components that counteract destabilizing motions during burst fire.

The modeling process involves simulating the weapon's behavior both with and without a muzzle device, allowing for the calculation of necessary compensatory impulses. An optimization procedure is then used to determine the parameter values that minimize muzzle displacement at critical firing moments. The methodology is validated through experimental testing on a specific type of portable automatic rifle, using a fixed mount and automated trigger system to isolate mechanical effects from human interference. The experimental results show close agreement with the model's predictions, confirming its accuracy and practical utility.

This study contributes a validated, physics-based approach for the design of muzzle devices as passive stabilizers in automatic rifles. It enables precise structural tuning to improve burst-fire accuracy, offering a technically feasible solution for enhancing firearm performance without relying on active systems or major structural redesigns.

2. THE PROBLEM OF DETERMINING STRUCTURAL CHARACTERISTICS OF THE MUZZLE DEVICE TO ENSURE GUN STABILITY

2.1 Assumptions

- Considering the gun as a multi-body system, the gun's

parts are considered to be absolutely rigid bodies when firing (except for springs)
- The distributed mass of the gun is replaced by the concentrated mass and the inertia moment located at the center of mass of the objects in the system
- The working parts are considered as material points with mass located at the center of mass, having plane-parallel motion to the gun body;
- The action of the shooter on the gun is modeled as a viscoelastic coupling with coefficients *K* and *C*.
- The forces acting on the gun are considered independent.

2.2 Physical Model

Consider the physical model of the motion of an assault rifle resting on the shoulder when firing as shown in Fig. 1.

In the above model: object 1 - the shooter's shoulder is simulated as a concentrated mass m_1, the force acting on the gun is converted to the resistance force with stiffness coefficient *K* and viscous coefficient *C*; object 2 - the gun body has mass m_2; object 3 - the moving part has mass m_3.

Coordinate systems: fixed coordinate system $O_0X_0Y_0Z_0$ has origin O_0 located at the initial shoulder rest point; dynamic coordinate system $O_1X_1Y_1Z_1$ is attached to object 1, has origin O_1 as the shoulder rest point; dynamic coordinate system $O_2X_2Y_2Z_2$ is attached to object 2, has origin O_2 as the coordinate of the center of mass of object 2; dynamic coordinate system $O_3X_3Y_3Z_3$ attached to object 3, with origin O_3 being the coordinate of the center of mass of object 3, due to the structure of the gun, axis O_3X_3 is parallel to O_2X_2 (parallel to the barrel axis).

Independent generalized coordinates: object 1 has 3 translational movements $\{q_1,q_2,q_3\}$ along the axes O_0X_0, O_0Y_0, O_0Z_0; object 2 has 3 rotational movements $\{q_4,q_5,q_6\}$ around the axes O_1X_1, O_1Y_1, O_1Z_1; object 3 has translational displacement $\{q_7\}$ compared to object 2 (O_2X_2).

The vector of generalized coordinates is determined by:

$$\vec{q} = \left(q_j\right)^T \ (\mathrm{j}=1\div 7) \tag{1}$$

However, the movements q_2, q_3 are very small and can be ignored when calculating the case of an assault rifle resting on the shoulder when firing.

2.3 Determining Structural Characteristics of the Muzzle Device

The system of Lagrange's differential equations of type II describes the motion of the system:

$$\frac{d}{dt}\left(\frac{\partial T}{\partial \dot{q}_j}\right) - \frac{\partial T}{\partial q_j} = Q_j \ (\mathrm{j}=1\div 7) \tag{2}$$

The total kinetic energy of the mechanical system is determined by the expression:

$$T = \sum T_i \quad (i=1\div 3) \tag{3}$$

In which, kinetic energy of object 1:

$$T_1 = \frac{1}{2}\dot{\vec{R}}_1^T \left[M\right]_1^{RR} \dot{\vec{R}}_1 \tag{4}$$

Kinetic energy of object 2:

$$T_2 = \frac{1}{2}\dot{\vec{R}}_2^T \left[M\right]_2^{RR} \dot{\vec{R}}_2 + \frac{1}{2}\vec{\omega}_2^T \left[A\right]_{20}\left[J\right]_2\left[A\right]_{20}^T \vec{\omega}_2 \tag{5}$$

Kinetic energy of object 3:

$$T_3 = \frac{1}{2}\dot{\vec{R}}_3^T \left[M\right]_3^{RR} \dot{\vec{R}}_3 + \frac{1}{2}\vec{\omega}_3^T \left[A\right]_{30}\left[J\right]_3\left[A\right]_{30}^T \vec{\omega}_3 \tag{6}$$

Total possible work of the whole system:

$$\begin{aligned}\delta W = {} & \delta W\left(F_{bb}\right) + \delta W\left(F_{ed}\right) + \delta W\left(F_{md}\right) \\ & + \delta W\left(\Pi_{sp}\right) + \delta W\left(P_G\right) + \delta W\left(F_{sh}\right) \\ & + \delta W\left(R_p\right) + \delta W\left(M_2\right)\end{aligned} \tag{7}$$

The total possible work of the entire mechanical system in the Eqn. (7) can be written in the form:

$$\delta W = \left(\sum_{i=1}^{3} \vec{F}_i^T \cdot \frac{\partial \vec{r}_i}{\partial \vec{q}}\right) \cdot \delta\vec{q} \tag{8}$$

Generalized force:

$$Q_j = \sum_{i=1}^{3} \vec{F}_i^T \cdot \frac{\partial \vec{r}_i}{\partial q_j} \ (\mathrm{j}=1\div 7) \tag{9}$$

where: $\vec{F}_i; \vec{r}_i$ - the force; the vector determines the point where the force is applied.

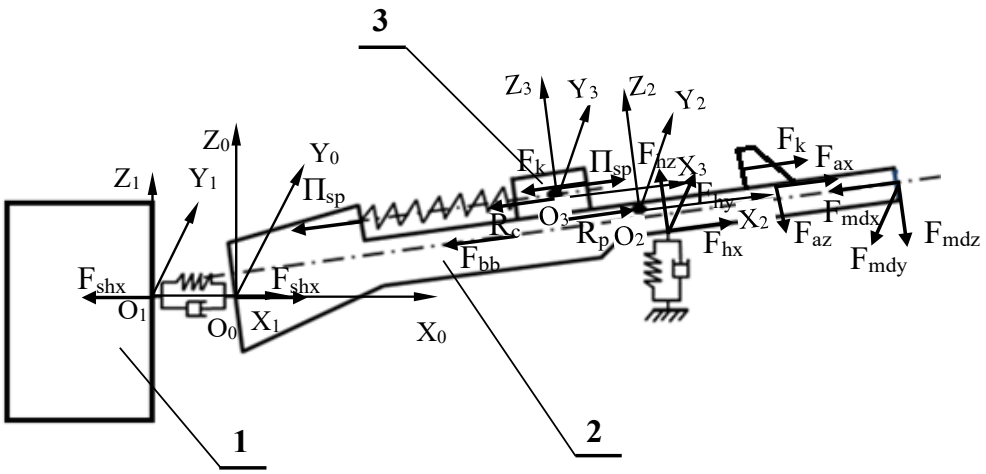

Figure 1. Model of gun movement.

Solving the displacement problem of an assault rifle without using the muzzle device (Eqn. (2)), we can determine the movement of the muzzle point $\vec{q}(iT)$. With desire for the rifle to be stable when firing the i+1st bullet in the series (i=1,2,…), that is, the position of the rifle when firing the i+1st bullet must return to the initial equilibrium position, the muzzle device must create a force $\vec{F}_{md}\ t)$, acting on the rifle to cause a movement $\vec{q}'(iT)$ that compensates for the movement of the rifle $\vec{q}\ iT)$ created by other forces according to the principle of additive effects. That is as follows:

$$\vec{q}'(iT) = -\vec{q}(iT) \tag{10}$$

Assuming that the forces acting on the rifle are considered independent, the muzzle device makes the rifle moves independently of the movement caused by the action of other forces. Therefore, only object 2 (gun, with mass m_g=m_2+m_{md}) is considered. The force exerted by the shooter on the rifle depends on the motion of the gun body, acting as a restoring force and a resistance force, so the shooter's impact still exists and is located at the point of contact between the shooter and the gun. The equation of translational motion in directions of the muzzle is established by applying Newton's second law:

$$M]\ddot{\vec{q}}_m + [C]\dot{\vec{q}}_m + [K]\vec{q}_m = \vec{F}_{md} \tag{11}$$

where: $\vec{q}_m = \left[q_{mx}, q_{my}, q_{mz}\right]^T$ - the vector of translational displacements of the muzzle in the three directions x, y, z.

The mass matrix, the damping matrix and the stiffness matrix are respectively defined by:

$$M] = \begin{bmatrix} m_g & 0 & 0 \\ 0 & J_g^{yy}/l_{md}^2 & 0 \\ 0 & 0 & J_g^{zz}/l_{md}^2 \end{bmatrix} \tag{12}$$

$$[C] = \frac{l_{O_2}^2}{l_{md}^2}\begin{bmatrix} C_x & 0 & 0 \\ 0 & C_{hy} & 0 \\ 0 & 0 & C_{hz} \end{bmatrix} \tag{13}$$

$$K\ = \frac{l_{O_2}^2}{l_{md}^2}\begin{bmatrix} K_x & 0 & 0 \\ 0 & l_{O_2}^2.K_{hy}/l_{md}^2 & 0 \\ 0 & 0 & l_{O_2}^2.K_{hz}/l_{md}^2 \end{bmatrix} \tag{14}$$

Muzzle force vector:

$$\vec{F}_{md} = \begin{bmatrix} F_{mdx} \\ F_{mdy} \\ F_{mdz} \end{bmatrix} = \begin{bmatrix} \alpha_T \\ \alpha_y \\ \alpha_z \end{bmatrix}.R_x \tag{15}$$

The muzzle force $\vec{F}_{md}(t)$ is a non-harmonic but periodic force, with a period T_0 equal to the period of the shot. This force begins to act on the gun at the moment the bullet passes through the muzzle cross-section and acts within a very short time t_f compared to the shot cycle. The effect of a force in a short time is expressed by its impulse value. With the force $\vec{F}_{md}(t$, it can be replaced by the impulse of the muzzle device J_f acting on the gun at time ξ (the moment the bullet passes through the muzzle cross-section).

$$J_f = \begin{bmatrix} \alpha_T \\ \alpha_y \\ \alpha_z \end{bmatrix}.\int_0^{t_f} R_x(\xi\ d\xi \tag{16}$$

The motion of the muzzle in the next process (at t >ξ) is a damped oscillation described by the general formula:

$$q_m(t\ =\ q_{mi}\ t \qquad (i = x, y, z) \tag{17}$$

where:

$$q_{mi}(t) = e^{-h_i(t-\xi)}. \left(\begin{array}{l} q_{mi}(\xi)\cos\bar{k}_i(t-\xi) + \\ \dfrac{\dot{q}_{mi}(\xi) + h_i q_i(\xi)}{\bar{k}_i}\sin\bar{k}_i(t-\xi) \end{array}\right) \tag{18}$$

with:

$$h_i = \frac{C_i}{2m_i},\ \bar{k}_i^2 = k_i^2 - h_i^2,\ k^2 = \frac{K_i}{m_i}$$

On the other hand:

$$m_i\dot{q}_{mi}(t) = \int_0^{t_f} P_{mdi}(\xi)d\xi = J_{fi} \tag{19}$$

We then get:

$$q_{mi}(t) = e^{-h_i(t-\xi)}. \left(\begin{array}{l} q_{mi}\ \xi)\cos\bar{k}_i(t-\xi) + \\ J_{fi}/m_i + h_i q_i(\xi) \\ \dfrac{}{\bar{k}_i}\sin\bar{k}_i(t-\xi) \end{array}\right) \tag{20}$$

From the Eqn. 10 and Eqn. 20, we can determine the impulse value J_f of the muzzle device. According to the Eqn. (16), we can determine the structural characteristics α_T, α_y, α_z of the muzzle device.

2.4 Algorithm to Solve Equation

The problem of gun motion to evaluate its stability is solved by Maple software. Based on solving the system of internal ballistic equations to determine the applied forces, we solve the system of motion equations. With the gun motion Eqn., we can determine the position of the muzzle at the time when the bullet leaves the barrel. Assigning these values to the gun motion caused by the muzzle force, we determine the characteristics of the muzzle device. Figure 2 shows a flowchart of the algorithm for determining the characteristics of the muzzle device.

2.5 Experimental Setup

The experimental equipment includes an assault rifle mounted on a specialized rack. This rack has an elastically connected recoil block to limit errors due to the shooter's operations while ensuring the most realistic description in normal shooting conditions. The gun is fired using an indirect trigger puller, ensuring that the trigger force is an internal force (for the gun), thereby eliminating unwanted effects of the shooter on the gun. This ensures the same conditions for all tests (Fig. 3).

In Fig. 4, the measuring object is depicted in its standard configuration. The TML Transducer CDP-25 displacement sensor is rigidly mounted on a rectangular bracket, oriented perpendicularly to the barrel axis and positioned directly behind the front sight base. This sensor remains stationary during firings. The CDP-25 features a measurement range of 0÷25 mm and a sensitivity of 500×10^{-6} mm^{-1}. A stop plate, which interfaces with the sensor's probe head, consists of two orthogonal planes and is affixed to the barrel head, thereby moving in unison with the gun barrel. A LB-3K force sensor

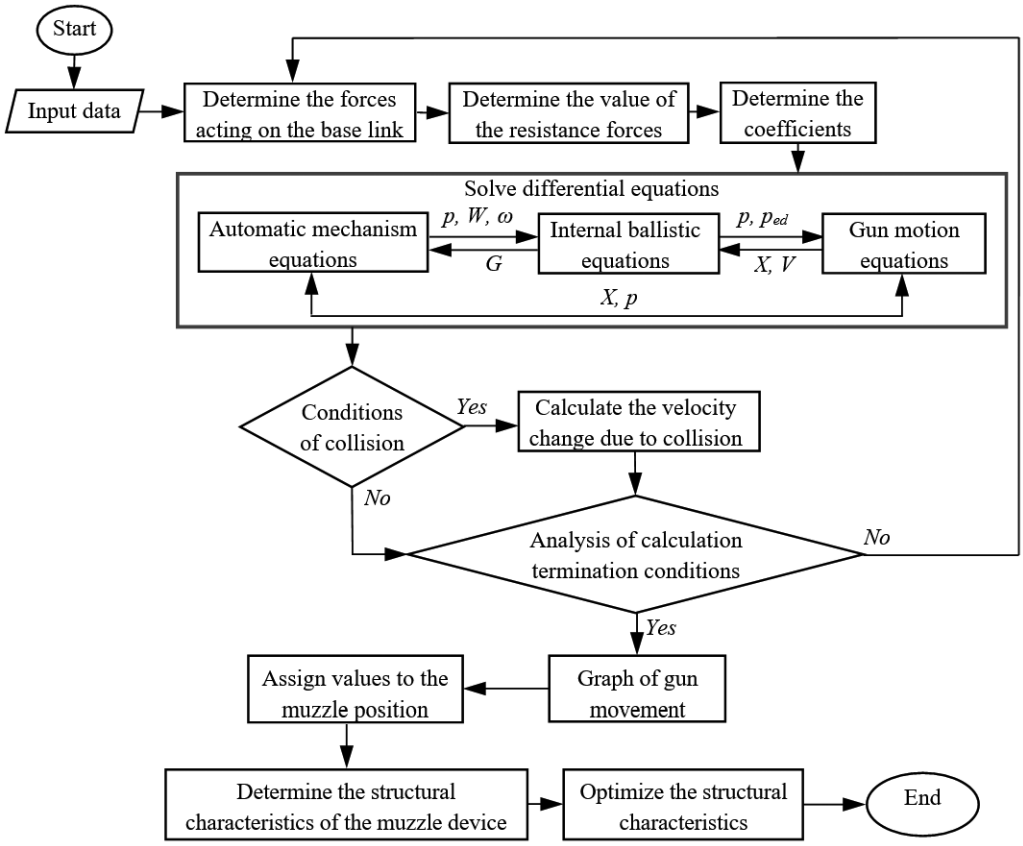

Figure 2. Flow chart for determining the characteristics of the muzzle device.

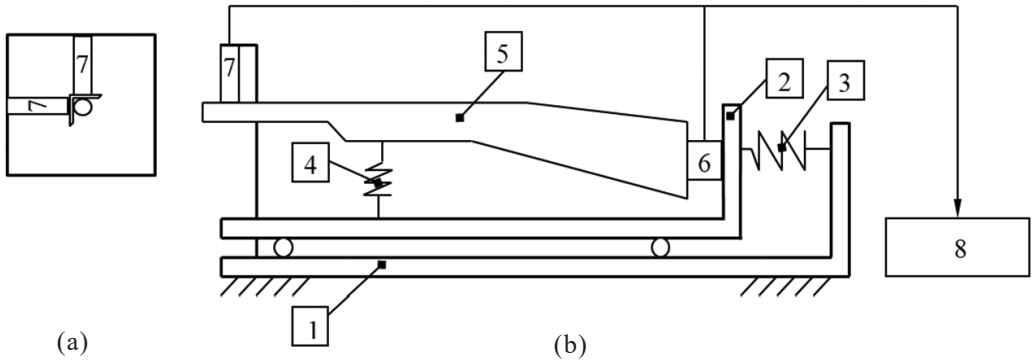

Figure 3. Block diagram of the measurement system; 1. Fixed rack; 2. Recoil block; 3. Shoulder compliance spring; 4. Hand compliance spring; 5. Measuring object; 6. Force sensor; 7. Displacement sensor; 8. Signal processing and display device. (a) In a cross-sectional plane orthogonal to the barrel axis at the sensor installation location; and (b) In the firing plane.

is installed behind the gun stock to measure recoil force along the barrel's axis. This sensor has a measurement capacity of 0÷3000 lbs and a non-linearity of 0.08 %. The mechanical parameters of the test setup are as follows: the support frame has dimensions of 900 mm ×250 mm ×760 mm and a mass of 94 kg, and is rigidly anchored to the floor. The recoil block has a mass of 20 kg, with associated spring stiffness values of 1600 N/m for the recoil block and 55 N/m for the oscillating frame.

Measurement signals are transmitted to a NI data acquisition system. Signal conditioning is performed using an SCXI-1520 module, and data is transferred to a computer via an SCXI-1600 module, with both modules housed within an SCXI-1000 chassis. Data acquisition and processing are managed using LabVIEW software, which enables the development of customized measurement programs through modular graphical blocks. Built-in signal filtering functions are employed to suppress noise and enhance the accuracy of the recorded data. Graphical output of the measurement results is displayed in real time.

3. RESULTS AND DISCUSSION

The internal ballistic and dynamic characteristics of the 7.62×39 mm assault rifle system, in conjunction with the structural parameters of the muzzle device, were used to simulate and evaluate the weapon's stability during burst fire. The critical design challenge is to determine the structural

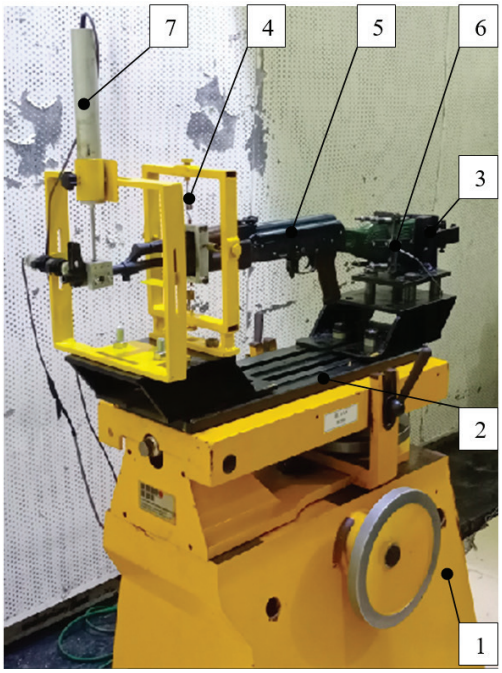

Figure 4. Experimental setup for measuring muzzle vibration and recoil force.

coefficients of the muzzle device that minimize muzzle displacement while managing recoil.

Two primary sets of structural coefficients (α_T, α_y, and α_z), representing the impact directions of the muzzle device's reactive forces, were evaluated (Table 1):

Option 1: Designed to restore equilibrium at the second shot.

Option 2: Designed to restore equilibrium at the third shot.

These results indicate a trade-off: compensating for muzzle deviation at one shot leads to deviation in the other. In both cases, the force component along the barrel axis (F_{mdx}) could not adequately counteract the recoil, revealing the inherent limitation of purely passive compensation along that axis. This confirms that structural asymmetry in the muzzle device (i.e., α_y and α_z) plays a critical role in lateral and vertical compensation but is insufficient for axial recoil mitigation. As a result, the automatic assault rifle is always subjected to recoil when firing. If the gun has a fixed barrel and rests against the shoulder when firing, the recoil force will be applied to the shooter's shoulder through the buttstock.

Table 2. Muzzle displacement and recoil force of the gun

Parameters		2nd shot	3rd shot
Recoil force (N)	R	182	180
Muzzle displacements (mm)	q_y	0.906	0.723
	q_z	-1.531	0.595

To ensure that the muzzle deviates from its equilibrium position at least at the moments when both the second and third bullets leave the barrel, some degree of deviation must be accepted $\{y,z\} \leq [y,z]$. By formulating and solving an optimization problem that minimizes deviations at both the second and third shots, an optimized structural coefficient set was found:

$$\alpha_T, \alpha_y, \alpha_z = 0.24, 0.09, 0.10$$

The resulting muzzle displacements and recoil forces at these critical moments, based on the refined muzzle design, are presented in Table 2.

These values illustrate a marked reduction in muzzle displacement, confirming that appropriately tuned structural coefficients, particularly those influencing lateral and vertical reaction forces, are key to enhancing weapon stability.

According to the preceding calculations, experimental measurements were conducted to validate the theoretical model. Figure 5 presents a snapshot of the measurement results captured directly from the display interface. To facilitate a clearer comparison between configurations with and without the muzzle device, the recorded data were exported to an Excel file, and plotted together in a single graph, as shown in Fig. 6.

Despite the graphical comparison, the precise moment of bullet exit from the barrel could not be distinctly identified in the plot. Therefore, the corresponding measurement data were extracted from the Excel file, and organized into tabular format for clarity.

The experimental results closely aligned with theoretical predictions, exhibiting deviations within an acceptable error margin of less than 10 %. Table 5 presents a direct comparison between the theoretical calculations and the measured values.

Minor discrepancies observed are primarily attributed to simplifications in the modeling process-such as the assumption of rigid-body dynamics and linear damping-as well as limitations inherent to the experimental setup, including sensor resolution and fixture tolerances. Nevertheless, the strong correlation between theoretical and experimental results

Table 1. Values of structural coefficients of the muzzle device

Option	Structural coefficient	Value	Muzzle deviation at 2nd shot	Value (mm)	Muzzle deviation at 3rd shot	Value (mm)
	α_T^1	#	q_x^{2nd}	0	q_x^{3rd}	
1	α_y^1	0.061	q_y^{2nd}	0	q_y^{3rd}	0.00161
	α_z^1	0.071	q_z^{2nd}	0	q_z^{3rd}	0.00314
	α_T^2	#	q_x^{2nd}		q_x^{3rd}	0
2	α_y^2	0.114	q_y^{2nd}	-0.00165	q_y^{3rd}	0
	α_z^2	0.134	q_z^{2nd}	-0.00325	q_z^{3rd}	0

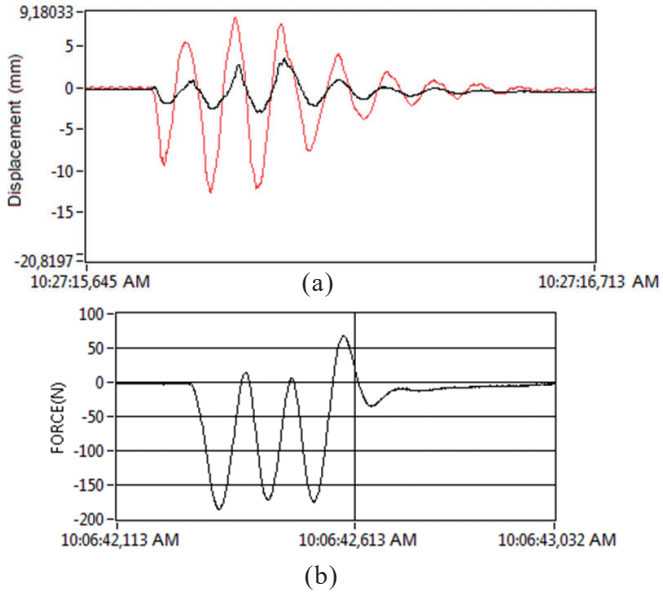

Figure 5. Measurement results when firing a series of 3 rounds with the muzzle device; (a) Muzzle displacements; (b) Recoil force.

supports the validity and predictive accuracy of the proposed model.

4. CONCLUSIONS

This study presents a comprehensive method for determining the structural characteristics of a muzzle device aimed at enhancing the stability of an assault rifle during short burst firing. The proposed approach is grounded in a solid mechanical foundation - applying the principle of independent force action and utilizing a nonlinear dynamic model that accounts for the complex interactions between internal ballistic forces, shooter dynamics, and structural recoil responses.

The analysis clearly demonstrates that the shape and orientation-dependent coefficients of the muzzle device (specifically α_T, α_y and α_z) play a critical role in compensating for vertical and lateral muzzle deviations. These parameters

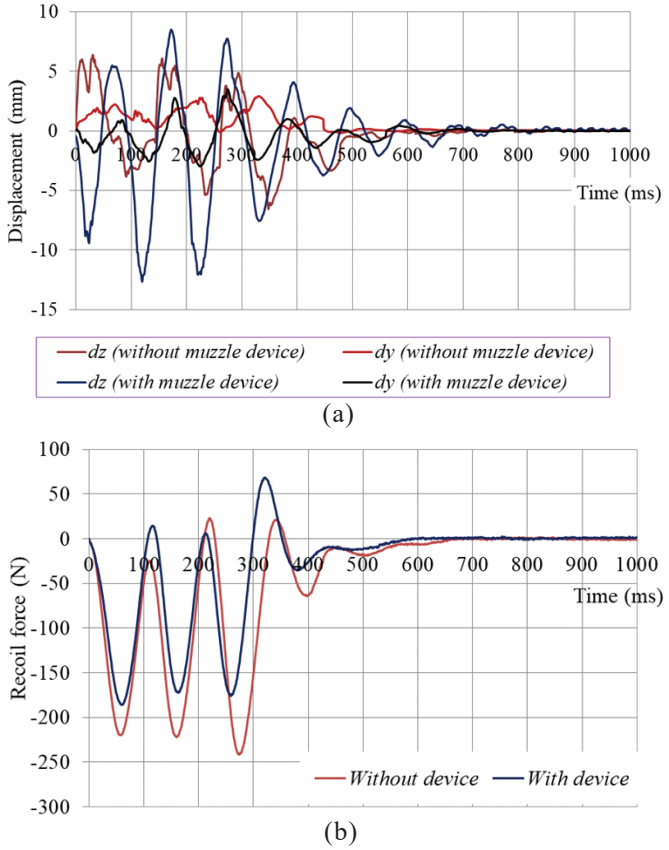

Figure 6. Measurement results when firing with and without the muzzle device; (a) Muzzle displacements; and (b) Recoil force.

allow for targeted manipulation of the reactive forces generated by propellant gases escaping from the barrel, which in turn generate stabilizing torques that counteract undesired muzzle movements.

By modeling the gun as a multi-body dynamic system and employing Lagrange's equations, the study successfully quantifies the relationship between muzzle impulse forces and resulting muzzle displacements. Notably, the optimized

Table 3. Results of recoil force measurement at the buttstock

Case	Shot	Times measured					$\bar{X}$ (N)	σ_X^*	ΔX	γ (%)
		1	2	3	4	5				
Without muzzle device	1st	-220	-233	-226	-220	-238	-227	3.57	13	1.57
	2nd	-221	-230	-234	-222	-240	-229	3.60	14	1.57
	3rd	-239	-228	-231	-241	-240	-236	2.63	10	1.12
With muzzle device	1st	-185	-181	-186	-174	-167	-179	3.59	14	2.01
	2nd	-172	-185	-187	-167	-178	-178	3.79	14	2.13
	3rd	-175	-184	-179	-171	-182	-178	2.35	9	1.32

Table 4. Displacement measurement results according to selected option

Shot	Muzzle displacements	Times measured					$\bar{X}$ (mm)	σ_X^*	ΔX	γ (%)
		1	2	3	4	5				
2nd	Vertical	-1.75	-1.69	-1.58	-1.78	-1.69	-1.698	0.03	0.13	2.0
	Horizontal	0.95	0.83	0.86	1.03	0.97	0.928	0.04	0.14	4.0
3rd	Vertical	0.52	0.56	0.64	0.63	0.73	0.616	0.04	0.14	5.9
	Horizontal	0.66	0.67	0.78	0.84	0.62	0.714	0.04	0.16	5.8

Table 5. Comparison of theoretical results and the experimental values

Results	2nd shot			3rd shot		
	Vertical displacement (mm)	Horizontal displacement (mm)	Recoil force (N)	Vertical displacement (mm)	Horizontal displacement (mm)	Recoil force (N)
Theoretical	-1.531	0.906	-182	0.595	0.723	-180
Experimental	-1.698	0.928	-178	0.616	0.714	-178
Error (%)	9.8	2.4	2.2	3.4	1.3	1.1

structural configuration of the muzzle device, obtained via a numerical solution and refinement process, significantly reduces both the recoil force and the deviation of the muzzle at critical instants, specifically when subsequent bullets exit the barrel in a burst.

Experimental validation confirmed the theoretical model's effectiveness, with error margins below 10 %, which are acceptable in practical weapons engineering. These results not only validate the predictive capacity of the proposed model but also highlight its practical value for the design and optimization of muzzle devices across various firearm platforms.

REFERENCES

1. Pathak A, Brei D, Luntz J, Lavigna C. A dynamic model for generating actuator specifications for small arms barrel active stabilization. *In* Proceedings Volume 6166, Smart Structures and Materials 2006: Modeling, Signal Processing, and Control; 61660D, 2006. doi: 10.1117/12.659175.
2. Garayev AZ, Meshcheryakov SM, Neverov AI. The Influence of the Operating Mode of Automatic Blowback Submachine Guns on the Efficiency of Fire. Technical Sciences, Izvestiya Tula State University, 2018, pp. 279-284 (Russian).
3. Sufiyanov VG, Nefedov DG, Klyukin DA. Results of Mathematical Modeling of Longitudinal-Transverse Oscillations of the Barrel in a One-Dimensional Statement Taking into Account the Influence of Internal. *In* Ballistic Processes, "Innovation Exhibition - 2020": Collection of Materials of the XXX Republican Exhibition-Session of Student Innovation Projects, Izhevsk, 2020, pp. 190-195 (Russian).
4. Kang KJ, Gimm HI. Numerical and experimental studies on the dynamic behaviors of a gun that uses the soft recoil system. *J. Mech. Sci. Technol*., 26, 2012, pp. 2167-2170.
5. Wang ZhQ et al. Optimization of Dynamic Characteristics of Automatic-Firing Muzzle with Damping. International Journal of Performability Engineering, 2019, 15(1): 1-12. doi:10.23940/ijpe.19.01.p1.112.
6. Ding Y, Zhou K, He L, Yang H. Experimental research on the muzzle response characteristics of small unmanned ground vehicles with small arms. *In* Proceedings of the Institution of Mechanical Engineers, Part C: Journal of Mechanical Engineering Science. 2021;236(9):4660-4670. doi:10.1177/09544062211057045.
7. Qing OY, Zheng JJ, Li ZC. Controllability analysis and testing of a novel magnetorheological absorber for field gun recoil mitigation. *Smart Mater, Struct*, 25, 115041, 2016.
8. Qiu M, Si P, Song J and Liao Z. Recoil Reduction Method of Gun with Side to Rear Jet Controlled by Piston Motion. Symmetry 2021, 13, 396, 2021. doi: 10.3390/sym13030396.
9. Ma L et al. Study on Micro Recoil Mechanism of the Weapon with a Nozzle and Two Chambers Separated by a Partition. *Journal of Physics: Conference Series*, Volume 2097, 2021 International Conference on Fluid and Chemical Engineering (ICFCE 2021), Wuhan, China, 2021. doi: 10.1088/1742-6596/2097/1/012009.
10. Liu Q et al. Effect of an Internal Impact Balance Mechanism on the Perceptible Recoil of Machine Gun. *Web of Conferences* 231, 03001, 2021. doi: 10.1051/e3sconf/202123103001.
11. Russell KA. Rifle Operating Group for Small Arms Recoil Reduction. Recent Patents in Mechanical Engineering, 6, 2013, pp. 194-199. doi: 10.2174/ 22127976113069990009.
12. Elnashar GA, Ashr MM. Design of Active Stabilization Controller for Tactical Rifle. *In* Proceedings of the 7th ICEENG Conference, Egypt, 2010.
13. Ramadhana MA et al. The Analysis of the Development of Muzzle Brake Design on SL Rifle 41. International Journal of Humanities Education and Social Sciences, 2024, 3(4). doi: 10.55227/ijhess.v3i4.780.
14. Nguyen DV, Bui VQ. The effect of muzzle devices on the distribution of muzzle waves when firing an assault rifle. Archive of Mechanical Engineering, vol. 71, No 3, 2024, pp. 445-466. doi: 10.24425/ame.2024.151332.
15. Vo VB, Nguyen DP, Nguyen MP. Study of the Effect of Some Muzzle Device Types on the Firing Force and Firing Impulse. Archives of Advanced Engineering Science, 2(4), 2024, pp. 224-231. doi:10.47852/bonviewAAES32021349.
16. Pemcak I, Novackova K, Balaz T, Krejci J & Bulinova I. Measurement of Flash Intensity at the Muzzle of a Firearm and Possible Protection against its Effects. Advances in Military Technology, 19(2), 2024, pp. 253-267. doi: 10.3849/aimt.01843.
17. Ahmed NZ et al. Analytical and experimental investigation of the muzzle brake efficiency. Mechanical Engineering, 2023. doi: 10.22190/ FUME220418028A.
18. Trebinski R et al. Investigations on influence of rifle automatic system action on values of energetic efficiency

coefficient of muzzle brakes. Defence Technology 18, 2022, pp. 1741-1747.
doi: 10.1016/j.dt.2021.06.003.
19. Perun P. Vibration small arm barrel, *University Review*, Vol. 13, No. 3, 2019. pp. 16-22.
20. Hua H, Liao Z, Zhang X. Muzzle Dynamic Characteristics Analysis and Its Matching for Firing Accuracy Improvement. Journal of Vibration and Shock, 36(8), 2017, pp. 29-33.
doi: 10.13465/j.cnki.jvs.2017.08.005.
21. Zhao X, Lu Y. A Comprehensive Performance Evaluation Method Targeting Efficiency and Noise for Muzzle Brakes Based on Numerical Simulation. Energies, 2022, 15(10), 3576.
doi: 10.3390/en15103576.
22. He F, Dai J, Lin S, Wang M, Su X. High-efficiency and low-hazard artillery recoil reduction technology based on barrel gas reflection. Sci Rep. 2024 Mar 29;14(1):7497.
doi: 10.1038/s41598-024-58313-2.
23. Liu Y, QU PU, Li Q. CFD-based numerical simulation and experiments for the optimization of dual-chamber gun muzzle retractor, June 2023.
doi: 10.21203/rs.3.rs-3085490/v1.
24. Zhao X, Lu Y. Multi-objective optimization of a muzzle brake to enhance overall performance. AIP Advances, 13, 085020, 2023.
doi: 10.1063/5.0145731.
25. Liu JB, Huang HSh, Zhu WF, Liu Y and Zhang L. Research on high efficiency muzzle brake technology of small caliber automatic gun. *In* J. Phys.: Conf. Ser. 1507 032003, 20-24 April 2020, Nanjing, China.
doi: 10.1088/1742-6596/1507/3/032003.
26. Phan KC. An Experimental Study of an Intelligent Muzzle Brake. *In* Brun, R., Dumitrescu, L.Z. (eds) Shock Waves @ Marseille III. Springer, Berlin, Heidelberg, 1995.
doi: 10.1007/978-3-642-78835-2_64.
27. Wang B, Heng G, and Wang D. Study on experiment measurement method of braking force of muzzle brake for vibration analysis. Vibroengineering PROCEDIA, 2018, Vol. 20, 179–184.
doi: 10.21595/vp.2018.20131
28. Abu-Elkhair MS, Sherif HA, Said SM. Experimental investigation of recoil force for automatic small arms and the effect of using muzzle brake. *In* International Conference on Aerospace Sciences and Aviation Technology, 2001; 9(ASAT Conference, 8-10 May 2001): 1-7.
doi: 10.21608/asat.2001.24832.

ACKNOWLEDGEMENT

This work was funded by the Research Fund of Le Quy Don Technical University under grant 24.1.26.

CONTRIBUTORS

Dr Dung Van Nguyen obtained his PhD in Engineering Mechanics from Le Quy Don Technical University and working as Head of the Department of Special Equipment, Le Quy Don Technical University of Vietnam. His research interests include: Artillery system design, weapon dynamics, and equipment development research.
In this study, he conceptualized and designed the research framework, conducted a comprehensive literature review.

Dr Viet Quy Bui obtained his PhD in Engineering Mechanics from Le Quy Don Technical University. He is currently a Senior Lecturer in the Department of Special Equipment at Le Quy Don Technical University. His research focuses on: Aerodynamic processes, automatic weapon dynamics, and equipment manufacturing and exploitation.
In this study, he contributed to model construction, calculations and data analysis.

Dr Trung Viet Nguyen obtained his PhD in Mechanical Mathematics from Tula Artillery Engineering Institute. He currently serves as the Leader of the Field Laboratory at Quy Don Technical University. His research interests include: Artillery system design, system integration, equipment reliability.
In this study, he established the experimental model and was responsible for collecting and processing experimental data.

Dr Huy Quang Mai obtained his PhD in Mechanical Engineering from Le Quy Don Technical University and working as a Vice Rector of Le Quy Don Technical University. His research interests include: Ballistics, equipment simulation, and optimization.
In this study, he contributed to methodology development and directed the research.